Pure & Appl. Chem., Vol. 49, pp. 905 - 913. Pergamon Press, 1977. Printed in Great Britain.

DENSITY FLUCTUATIONS IN AMORPHOUS AND SEMICRYSTALLINE POLYMERS

W. Ruland

Fachbereich Phys. Chemie, Universität Marburg, Lahnberge, Gebäude H
D - 3550 Marburg

Abstract

The small-angle scattering of amorphous and semicrystalline polymers contains an intensity component related to density fluctuations (Fl) within the crystalline and amorphous domains. A quantitative study of this parameter results in information on the changes of thermal motion and disorder as a function of temperature, crystallinity and preferred orientation.

Amorphous polymers show a change of slope of the Fl - T-curves at T_g. Above T_g the value of Fl corresponds to the relationship valid for a system in thermodynamic equilibrium, below T_g the Fl - T-curve tends towards a non-zero value at $0^{\circ}K$ with decreasing slope. At very low temperatures the value of Fl can be considered a sum of the contributions from the "frozen-in" disorder and from phonons of long wave-length.

Semicrystalline polymers show Fl - T-curves similar to those of amorphous polymers. At a given temperature Fl shows an approximately linear decrease with increasing crystallinity.

Preferred orientation produces an anisotropy in the diffuse small-angle scattering related to the density fluctuations which can be interpreted in terms of an anisotropy of the phonon velocities. The temperature dependence of this anisotropy can be used to estimate the phonon velocities involved.

INTRODUCTION

The fact that the scattering intensity extrapolated towards zero angle is proportional to the density fluctuations has been known for a long time (Ref.1). For X-ray scattering, considering the electron density as the basic structural parameter, one obtains

$$\lim_{\theta \to 0} \frac{1}{N} I_{e.u.} = \frac{\langle N^2 \rangle - \langle N \rangle^2}{\langle N \rangle} = Fl_{el} \qquad (1)$$

where $I_{e.u.}$ is the scattering in electron units, N the number of electrons in the irradiated volume and Fl_{el} the fluctuation of the electron density. If the sample is composed of N_M identical particles (molecules) with Z_M electrons per particle, the particle density fluctuation Fl_M is given by

$$Fl_M = \frac{1}{Z_M} Fl_{el} \quad .$$

It has been shown in an earlier paper (Ref.2) that the limit $\theta \to 0$ in eq. (1) has to be replaced by the integral

$$Fl(v_B) = \int_v \frac{1}{N} I \frac{1}{v_B} \bar{\Phi}_B^2 \, dv_s \qquad (2)$$

if the reference volume v_B in which the fluctuation of N is considered has to be taken explicitely into account. The existence of a limit in the sense of eq. (1) is equivalent to the existence of the limit

$$Fl = \lim_{v_B \to \infty} Fl(v_B) \quad . \qquad (3)$$

It has been shown (Ref 3,4 5) that the paracrystalline disorder model of Hosemann and Bagchi (5) cannot be used for the interpretation of homogenously disordered structures since the application of eq. (2) leads to fluctuation values which increase with v_B.

For one-component systems in thermodynamic equilibrium the particle density fluctuation Fl_M is given by

$$Fl_M = \rho_M kT \varkappa_T \qquad (4)$$

where ρ_M is the average particle density, k the Boltzmann constant, T the absolute temperature and $\varkappa_T$ the isothermal compressibility. Levelut and Guinier (6) have shown that quantitative measurements of the diffuse small-angle scattering of liquids in the sense of eq. (1) leads to values corresponding to eq. (4). In perfect crystals the thermal diffuse scattering (TDS) which is distributed all over the reciprocal space and has maxima near reciprocal lattice points produces a small-angle scattering which, for single crystals, is direction dependent and related to the group velocities v_l of long wave-length longitudinal lattice vibrations. In the harmonic approximation, this anisotropic small-angle scattering is given by

$$\lim_{s\to 0} \frac{1}{N} I_{e.u.}(\vec{s}) = \frac{\rho_{el} kT}{\rho_m} \frac{1}{v_l^2(\vec{e})} \qquad (5)$$

where $\vec{s}$ is the reciprocal space vector ($s = 2 \sin\theta / \lambda$), ρ_m the mass density and $\vec{e}$ the unit vector defining the direction of $\vec{s}$. Using eq. (2) and eq. (3) one can show that the density fluctuations in a perfect crystal are

$$Fl_{el} = \frac{\rho_{el} kT}{\rho_m} \left\langle \frac{1}{v_l^2} \right\rangle_\omega \qquad (6)$$

where $\langle\ \rangle_\omega$ stands for the spherical average.

In the case of imperfect crystals or glasses the density fluctuations should be higher than those of the equilibrium states due to the contribution of structural disorder.

EXPERIMENTAL

The dermination of the diffuse small-angle scattering in the limit $\theta \to 0$ according to eq. (1) involves an extrapolation of the intensity measured at moderately small angles ($1^o < \theta < 4^o$ for Cu-radiation) excluding the region at very small angles which contains the contribution of structural inhomogeneities due to voids or impurities in the case of amorphous samples and to the crystalline-amorphous superstructure in the case of semi-crystalline structures. It was found that log I - θ^2 plots produced linear relationships for the liquids used as standard samples as well as for the polymers studied (see Fig. 1) so that a reproducable extrapolation to $\theta = 0^0$ was possible.

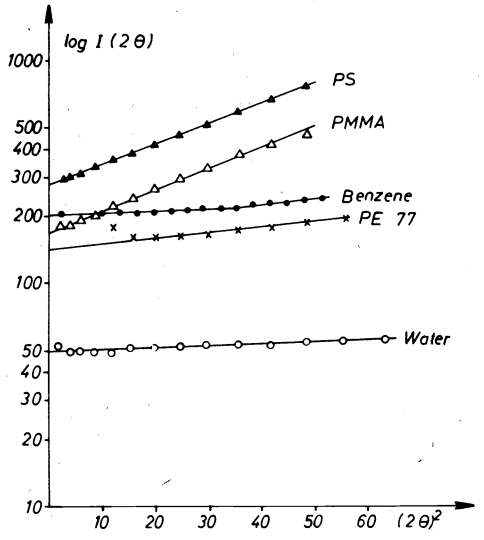

Fig. 1. Semilog plot of the intensity versus $(2\theta)^2$.

This procedure represents essentially an extrapolation of the small-angle part of the "amorphous halo" and the TDS-component of the crystalline interferences towards zero scattering angle. Since the intensity is, in general, very small in this region as compared to the wide-angle scattering in general as

well as to the small-angle scattering due to the crystalline - amorphous superstructure, the possibility of contributions from other scattering effects has to be checked very carefully. It was found that the main source of error is a contribution from multiple wide-angle scattering which can be eliminated by extrapolating the normalized intensity values measured at various sample thicknesses to zero thickness.

Normalization was achieved by measuring the diffuse small-angle scattering of water, benzene, cyclohexane and glycol, and computing the corresponding intensity in electron units with the help of eq. (1) and eq. (4). Figure 2 shows the temperature dependence of Fl_{el} for cyclohexane measured from 4°K to 300°K showing the discontinuity at the melting point as well as the phase transition at low temperatures.

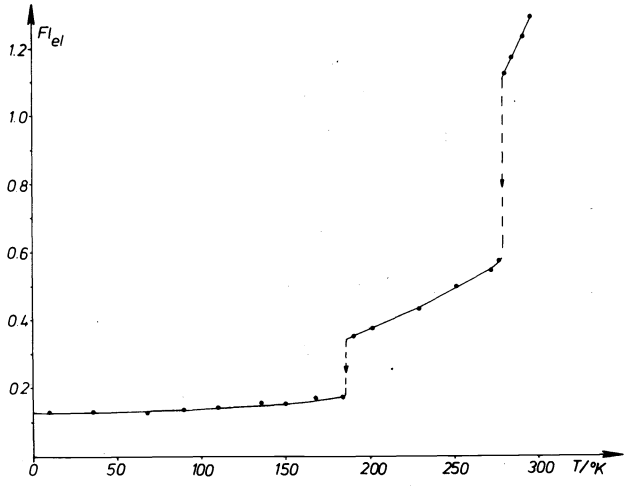

Fig. 2. Electron density fluctuation of cyclohexane as function of temperature.

AMORPHOUS POLYMERS

The temperature dependence of Fl_{el} obtained from the diffuse small-angle X-ray scattering (Ref. 7 and 8) is presented in figures 3 and 4 for atactic PMMA and polystyrene, respectively. Both curves show a change of the slope at T_g. Above this temperature the curve for PMMA corresponds to theoretical values calculated according to eq. (4) using $\varkappa_T$ values reported by Hellwege, Knappe and Lehmann (9), for polystyrene the corresponding theoretical values using $\varkappa_T$ values reported by the same authors are somewhat lower. In a temperature range from T_g down to about $T_g - 50^o$, the Fl - T -curves are roughly proportional to T. This behaviour has been explained by Wendorff and Fischer (10) on the basis of a theoretical treatment using non-equilibrium thermodynamics which results in a modification of eq. (4) in that the value of $\varkappa_T$ is taken as constant and equal to the value at T_g for temperatures below T_g. At lower temperatures Fl decreases gradually less rapidly with T and tends towards a non-zero value at 0°K. This value can be considered to represent the "frozen-in" disorder of the glassy polymer, the increase of Fl with increasing T can, at least at low temperatures, be explained by the contribution of long wave-length phonons to the thermal motion in this "frozen-in" disordered structure. The magnitude of this contribution can be assessed, to a first approximation, by a relationship of the type of eq. (6). In order to check the validity of this assumption, the longitudinal ultrasonic velocities (10 MHz) at low temperatures reported by Salinger (11), the longitudinal ultrasonic velocities (6 MHz) at moderate temperatures reported by Lamberson, Asay and Guenther (12) and the Brillouin scattering data (≃ 10 GHz) reported by Dietz and Wiggins (13), by Brody and Lubell (14) and by Friedmann, Ritger and Andrews (15) have been used to calculate the temperature dependent component of Fl according to eq. (6) and plotted together with the experimental data in figures 3 and 4. These data show that the assumption

$$Fl_{el}(T) = Fl_{el}(0) + \frac{\rho_{el}\, k\, T}{\rho_m\, v_l^2} \qquad (7)$$

appears to be valid for nearly the whole temperature range below T_g.
It is of interest to note that the values calculated from the ultrasound velocity at 6 MHz and the Brillouin scattering data corresponding to frequencies of about 10 GHz differ by only 2 % which indicates that the frequency dependence is, in this range of temperatures, negligible, and this justifies

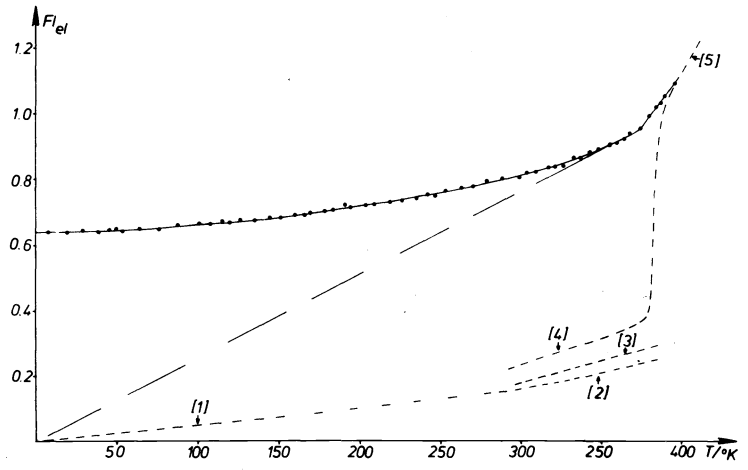

Fig.3. Electron density fluctuation of atactic PMMA as function of temperature. Curves [1]- [5] are calculated from: [1] longitudinal ultrasonic velocity data (Ref. 11), [2] Brillouin scattering data (Ref. 15), [3] Brillouin scattering data (Ref. 13) or longitudinal ultrasonic velocity data (Ref. 12), [4] isothermal compressibility (Ref. 9) and transversal ultrasonic velocity data (Ref. 12), [5] isothermal compressibility (Ref. 9).

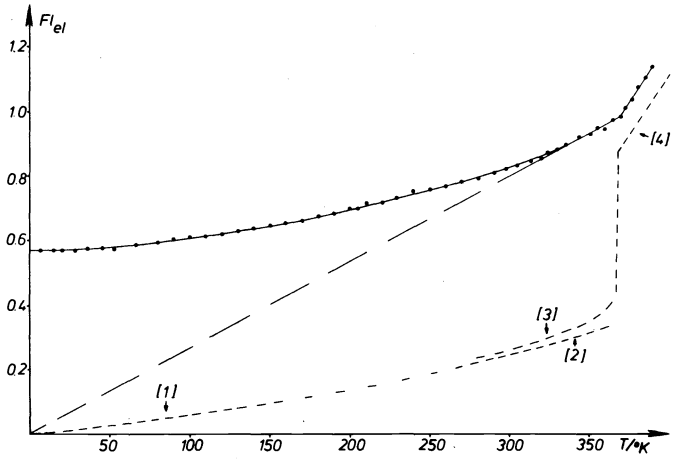

Fig.4. Electron density fluctuation of atactic polystyrene as function of temperature. Curves [1]- [4] are calculated from: [1] longitudinal ultrasonic velocity data (Ref. 11), [2] longitudinal ultrasonic velocity (Ref. 12) or Brillouin scattering data (Ref. 14), [3] isothermal compressibility data (Ref. 9) and transversal ultrasonic velocity data (Ref. 12), [4] isothermal compressibility data (Ref. 9).

also the comparison with values derived from X-ray scattering which - although the extrapolation to 0^{o} scattering angle is equivalent to an extrapolation to zero frequency - are nevertheless based on intensity measurements at scattering angles corresponding to far higher frequencies.
A further comparison can be carried out using the $\varkappa_T$ -values of Hellwege, Knappe and Lehmann (9) below T_g to calculate sound velocity values according to the relationship

$$\frac{1}{\rho_m v_l^2} = \frac{\varkappa}{1 + \frac{4}{3}\varkappa G} \qquad (8)$$

where G is the shear modulus. If the latter is taken from the transversal ultrasonic velocities reported by Lamberson, Asay and Guenther (12), a series of Fl-values can be calculated for temperatures

at and below T_g which should correspond to the contribution of thermal motion to Fl. At lower temperatures these values are slightly higher than the values calculated from ultrasound velocities probably due to the fact that $\varkappa_T$ has been used instead of $\varkappa_S$ required for eq. (8). The steep increase of these values at T_g can be taken as an indication that, at the glass temperature, a density fluctuation composed of a component due to thermal motion and a component due to "frozen-in" disorder changes to a density fluctuation entirely due to thermal motion. This change does, however, not involve a change of the total density fluctuation but only a change in the slope of the Fl-T -curve.
Comparing figures 2, 3 and 4 , the difference between glass transition and crystallization can be demonstrated in the schematic Fl-T-curves shown in figure 5.

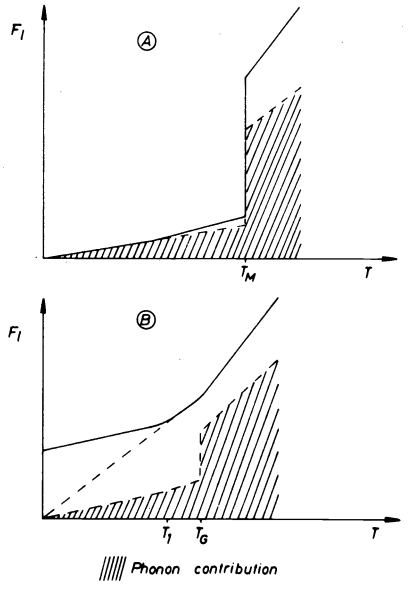

Fig.5. Schematic Fl - T -plots for crystallization (A) and glass transition (B).

At the melting point, both the total value of Fl and the phonon contribution increase discontinously, whereas at T_g, only the phonon contribution increases discontinously, the total value of Fl does not change due to a compensating decrease of the contribution due to the "frozen-in" disorder.

SEMICRYSTALLINE POLYMERS

In the case of semicrystalline polymers there exists, in general, a small-angle scattering due to the superstructure composed of crystalline and amorphous domains with an intensity several orders of magnitude higher than that due to the density fluctuations within the crystalline and amorphous domains. The small-angle scattering of the superstructure decreases, however, very rapidly with increasing angle so that it can be separated easily from the slowly increasing intensity of the scattering due to the density fluctuations by a proper choice of the angular region in which the intensity is measured (Ref. 7). Figure 6 shows Fl_{el} values measured for a series of polyethylene samples as a function of the crystallinity for various temperatures including values for $0^{\circ}K$ obtained by extrapolation.
For a given temperature the Fl values decrease linearly with increasing crystallinity which can be interpreted by a relationship of the type

$$Fl = x_a Fl_a + x_c Fl_c$$

where x_a and x_c are the fractions of amorphous and crystalline matter, respectively. This indicates that the density fluctuations in the crystalline and amorphous regions can be considered mutually independent. Eq. (9) permits thus an extrapolation towards $x_c = 1$ and $x_a = 1$ which results in the determination of Fl_c and Fl_a for various temperatures.

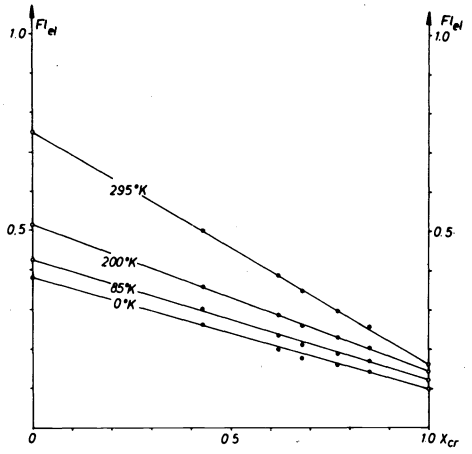

Fig. 6. Electron density fluctuation as a function of crystallinity and temperature.

Figure 7 shows a series of Fl_{el} - T -curves for polyethylene samples with varying crystallinity, including the extrapolated values of the Fl_c - T - and Fl_a - T -curves.

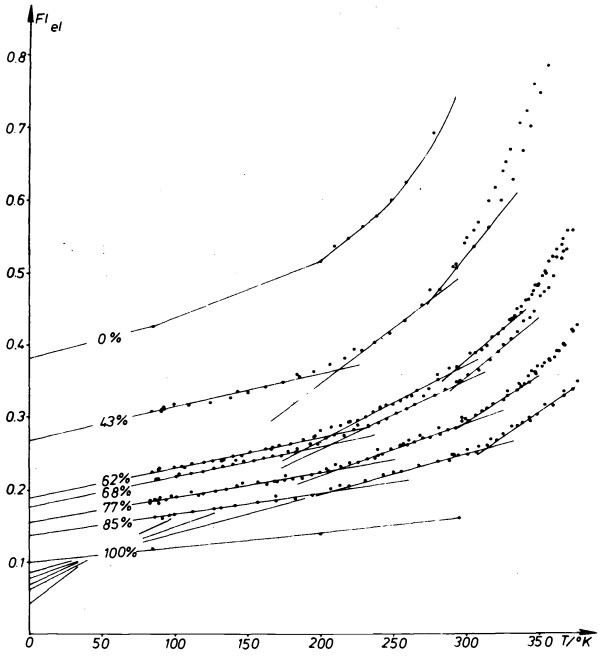

Fig. 7. Electron density fluctuation in polyethylene as a function of temperature and crystallinity.

The curves are very similar to the ones obtained for the amorphous polymers except for the rapid increase at temperatures approaching the melting point which are due to the decrease of the crystallinity in the melting region. All curves show a change of slope around 300°K comparable to that observed at T_g in the case of the amorphous samples. Making proper corrections for the fact that Fl_c is not zero at 0°K, one obtains a linear relationship of these apparent T_g values (called T_2 in the following) with x_c as can be seen in figure 8.
Another transition temperature can be defined, although less neatly, at the change of slope marking the limit between an Fl - T -relationship according to eq. (7) and the region in which the approximation

$$Fl = \rho k T \left(\varkappa_T \right)_{T_g}$$

proposed by Wendorff and Fischer (10) is valid for the amorphous regions. This temperature, called T_1, does not change with crystallinity, as can be seen in figure 8, and corresponds rather well to the "lower T_g" of PE defined by Boyer (17), whereas T_2 is about 60° higher than the "upper T_g"

defined by the same author, although its increase with crystallinity is similar.

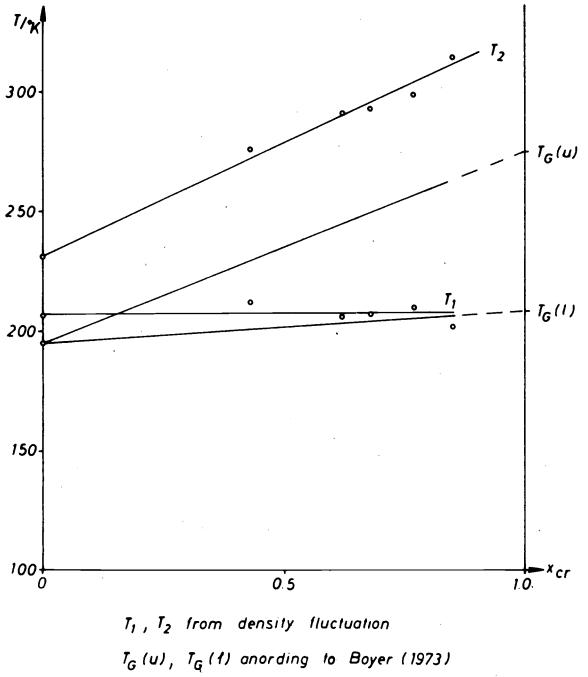

Fig. 8. Transition temperatures of PE as a function of crystallinity.

To understand the significance of the T_1 and T_2 values obtained from Fl-T-curves for semicrystalline polymers, more studies of this kind on other polymers have to be carried out. Preliminary results obtained for polypropylene (Ref. 8) show that also for this polymer the T_2 values obtained from Fl-T-curves are about 40° higher than the T_g values obtained by other methods, whereas T_1 is close to these T_g values.
Figure 9 shows the Fl-T-curve of polypropylene sample with a crystallinity of 60 % in which the change of slope at $T_1 = 260^{\circ}K$ and $T_2 = 300^{\circ}K$ is clearly visible.

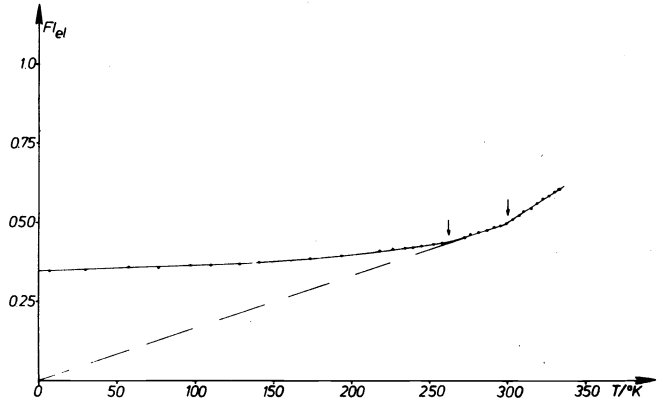

Fig. 9. Electron density fluctuation of polypropylene as a function of temperature.

Applying eq. (7) to calculate the velocities of long-wave-length phonons in the region below T_1 for the PE samples a series of v_l -values is obtained which are plotted in figure 10 together with the values obtained from the extrapolated Fl-T-curves for 0 % and 100 % crystallinity and ultrasonic velocities reported by Waterman (16). Even taking into account the error limits indicated in figure 10, there seems to be no reason for assuming a linear relationship between v_l and x_c.

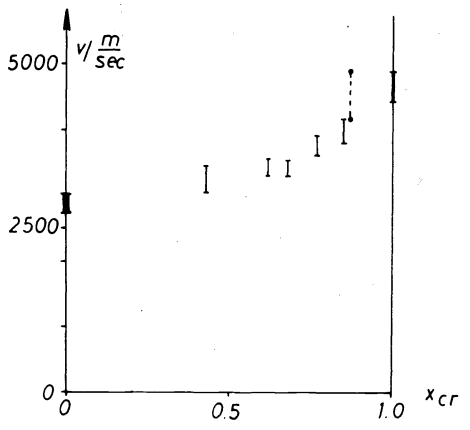

Fig.10. Velocity of long-wave-length phonons at low temperatures in polyethylene as a function of crystallinity. ——— from small-angle X-ray scattering; -·-·-·- extrapolated from ultrasonic measurements of Waterman (16).

ANISOTROPIC SAMPLES

In the case of anisotropic samples the TDS part of the small-angle scattering should be anisotropic and the scattering intensity extrapolated towards zero angle should be given by eq. (5). Studies on an uniaxially stretched PE film with a crystallinity of 56 % and an orientation parameter f = 0.540 for the chain axes in the amorphous regions and f = 0.936 for the crystalline c-axes show that such an anisotropy is actually observed (Ref.8). The results are presented in figure 11 as a function of the angle φ between the principal axis and the direction of the intensity measurement in reciprocal space for various temperatures.

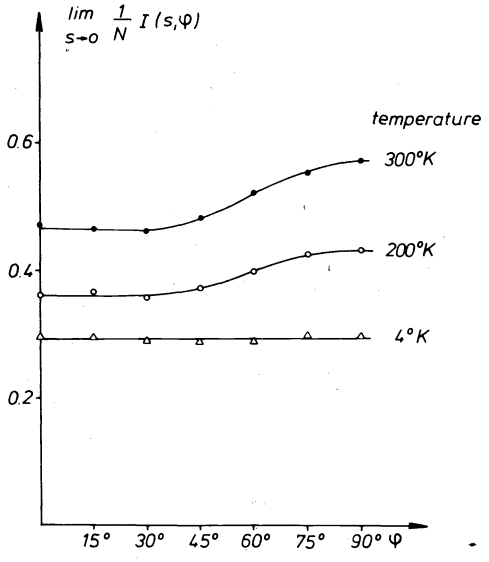

Fig.11. Anisotropy of the diffuse small-angle scattering extrapolated to zero angle as a function of φ for various temperatures (PE film).

One observes a decrease of the average value as well as of the anisotropy of this intensity with decreasing temperature. The values extrapolated to $0^{o}K$ indicate that no anisotropy is present in the scattering due to the "frozen-in" disorder although both the crystalline and the amorphous domains show a marked preferred orientation. This can only mean that the disorder in these domains is isotropic.
Subtraction of the intensity extrapolated to $0^{o}K$ from the intensity as a function of φ measured at higher temperatures results in the determination of the direction dependent v_l values for long-wavelength phonons which are plotted in figure 12.

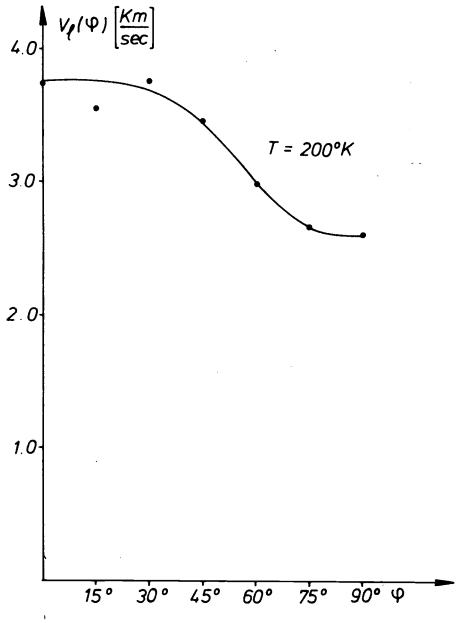

Fig. 12. Direction dependence of phonon velocities in a PE film.

Unfortunately, no ultrasonic or Brillouin scattering measurements are, at present, available to compair these results. One can expect however that such measurements will be of particular interest in the case of high modulus samples.

Acknowledgement
This work was supported by the Deutsche Forschungsgemeinschaft.

REFERENCES

1. F. Zernike and J.A. Prins, Z.Phys. 41, 184-194 (1927).
2. W. Ruland, Progr. Colloid & Polymer Sci. 57, 192-205 (1975).
3. R. Perret and W. Ruland, Koll.-Z.u.Z.Polym. 247, 835-843 (1971).
4. R. Brämer and W.Ruland, Makromol.Chem., in press.
5. R. Hosemann and S.N. Bagchi, Direct Analysis of Diffraction by Matter (Amsterdam 1962).
6. A.M. Levelut and A.Guinier, Bull. Soc. Minéral. Cristallogr. 40, 445-451 (1967).
7. J. Rathje and W. Ruland, Colloid & Polymer Sci. 254, 358-370 (1976).
8. W. Wiegand and W.Ruland, Verh. d. Deutschen Physikal. Gesellsch., Frühjahrstagung Bad Nauheim 1976.
9. K.H. Hellwege, W. Knappe and P. Lehmann, Koll.Z.u.Z.Polym. 183, 110-120 (1962).
10. J.H. Wendorff and E.W. Fischer, Koll.Z.u.Z.Polym. 251, 876-883 (1973).
11. G.L. Salinger, Amorphous Materials, Wiley, London, 475-485 (1972).
12. D.L. Lamberson, J. Asay and A.H. Guenther, J.Appl.Phys. 43, 976-985 (1972); J.Appl.Phys. 40, 1778-1783 (1968).
13. D.R. Dietz and T.A. Wiggins, J.Appl.Phys. 43, 3631-3636 (1972).
14. E.M. Brody and C.K. Lubell, J. Polymer Sci. 13, 295-301 (1975).
15. E.A. Friedmann, A.J. Ritger and R.D. Andrews, J.Appl.Phys. 40, 4243-4247 (1969).
16. H.A. Waterman, Koll.Z.u.Z.Polym. 192, 9-16 (1963).
17. R.F. Boyer, Macromol.Rev. 6, 288-299 (1973).